Phase separation in fully oxygenated $Y_{1-y}Ca_yBa_2Cu_3O_x$ compounds

E. Liarokapis,[1] D. Palles,[1] D. Lampakis,[1] G. Böttger,[2] K. Conder,[2] and E. Kaldis[3]
[1]*Department of Physics, National Technical University of Athens, GR-15780 Athens, Greece*
[2]*Laboratory for Neutron Scattering ETH and PSI, Villigen PSI, Switzerland*
[3]*Laboratorium für Festkörperphysik, ETH Zürich, CH-8093 Zürich, Switzerland*
(Received 8 March 2004; published 19 January 2005)

A micro-Raman spectroscopic study has been carried out on fully oxygenated $Y_{1-y}Ca_yBa_2Cu_3O_x$ (YBCO) compounds with $y=0.0-0.2$ and oxygen concentration varying with Ca in the range ($x\sim 6.960$ and 6.995). The spectral profiles of the $4A_g$ and $1B_{1g}$-like symmetry phonons show minor modifications with Ca, but two modes that appear close in energy to the in-phase and the out-of-phase phonons gain intensity with the Ca substitution. The changes in the intensity of these two satellite modes with the amount of Ca are correlated with modifications in the dimpling of the CuO_2 planes, as detected by extended x-ray absorption fine structure, and can be attributed to the formation of superstructures and to phase separation phenomena. The evolution of two bands in the in-phase phonon, associated in pure YBCO with local structural distortions and the coexistence of optimal and oxygen overdoped phases, remains completely independent of the Ca concentration. It appears that the Ca atoms have the tendency to be surrounded by Y atoms forming an independent nanophase of the type $Y_{0.5}Ca_{0.5}Ba_2Cu_3O_x$ with the additional carriers from Ca not contributing to an excess doping of the system.

DOI: 10.1103/PhysRevB.71.014303 PACS number(s): 78.30.−j, 74.25.Kc, 74.62.Dh, 74.72.Bk

I. INTRODUCTION

Structural and electronic inhomogeneities constitute intrinsic properties of cuprate superconductors. In the $YBa_2Cu_3O_x$ (YBCO) superconductor doping by oxygen induces ordering of the chains with the ortho-II phase having a transition temperature of 60 K, and the optimally doped phase with $T_c=92$ K. The overdoping of YBCO presents preparational difficulties as oxygen cannot easily exceed the nominal optimal concentration $x=7$. The real optimal value for oxygen doping of YBCO is for $x=6.92$. A systematic study of YBCO in the oxygen overdoped region has revealed a coexistence of phases and two transition temperatures, which correspond to the optimal and overdoping phases. A Raman study has revealed a phase transition related with structural modifications in the CuO_2 planes[1] at the optimal to overdoped oxygen concentrations. The Raman study has shown that the phonon of A_g symmetry due to the in-phase vibrations along the c axis of the oxygen atoms O(2,3) at the CuO_2 planes decreases in energy with the addition of carriers and, beyond optimum oxygen doping, softens accompanied with a reduction in T_c.[2] A gap has been actually observed for $x>6.95$ in the distribution of the energy of this phonon, pointing out to the coexistence of phases in the overdoped region ($x>6.975$).[1] A similar behavior has been detected at low temperatures.[3]

The substitution of Ca for Y (yttrium) in YBCO has been used to produce an expected equivalent electronic system lying further into the overdoped region. This substitution was originally considered to follow the generally accepted scheme of the increase of carriers,[4] which of course is related with the amount of the oxygen concentration as well.[5]

In a systematic preparation and study of the $Y_{1-y}Ca_yBa_2Cu_3O_x$ compound with carefully controlled oxygen content,[6] magnetic measurements have shown the existence of two maxima in the curvature of the diamagnetic signal.[7] As in the case of overdoped YBCO, the higher transition temperature is only slightly reduced compared to the maximum T_c of the optimally doped phase, while, in contrast to the overdoped YBCO case, the lower transition temperature is strongly reduced with increasing overdoping.[7] X-ray and neutron diffraction studies of the same samples[8] revealed that some bond lengths such as the Cu(2)-O(2/3) dimpling vary strongly with Ca doping.[5] This dimpling shows the strongest change (0.9%) observed and is in support of the conclusion from neutron diffraction[8] and extended x-ray absorption fine structure (EXAFS) measurements in YBCO (Ref. 9) and $Y_{1-y}Ca_yBa_2Cu_3O_x$ that T_c follows the changes of this bond.[7] The above structural and electronic inhomogeneities support the existence of at least two phases. Further investigations of the same samples by Ca (Ref. 10) and Y (Ref. 11) EXAFS spectroscopy, which is a local structure probe, allowed a comparison with the neutron diffraction results[8] (average crystallographic structure probe). Very interesting is the dependence of the Cu(2)-O(2/3) dimpling on the Ca content: A two-steplike reduction in the dimpling is observed with EXAFS at approximately $y=7\%$ and 14% consistent with the neutron diffraction data.[8] This can be explained by the existence of two phases in the solid solution of $Y_{1-y}Ca_yBa_2Cu_3O_x$ due to monodisperse dissolution of Ca in the YBCO matrix: (a) a matrix of undistorted $YBa_2Cu_3O_x$ cells and (b) distorted $(Y\text{-}Ca)Ba_2Cu_3O_x$ crosslike clusters where Ca is surrounded by four nearest neighbor Y cells.[10] A process treating the distorted clusters as percolation centers may account for the observed dimpling discontinuities. The recent work on fully oxygenated $YBa_2Cu_3O_x$ indicates that appreciable local disorder phenomena may be expected in these compounds.[7,9–11]

In this work, samples from the same series of $Y_{1-y}Ca_yBa_2Cu_3O_x$ have been used. The oxygen content has been measured with high accuracy[6] and revealed an unusual correlation between oxygen content and Ca concentration.[5,7]

A Raman spectroscopic study of these samples has been carried out aiming to delineate the effect of the Ca substitution for Y in connection with the oxygen content behavior.[5,7,12]

II. EXPERIMENT

The samples used in this study were taken from the batches used in the above mentioned investigations,[5,7,8,10,11] where a series of fully oxygenated polycrystalline samples of $Y_{1-y}Ca_yBa_2Cu_3O_x$ ($y=0.00$, 0.02, 0.04, 0.05, 0.07, 0.09, 0.10, 0.12, 0.14, 0.15, 0.17, and 0.20) were prepared by solid state reaction.[8] Only the $y=0.20$ sample has shown small amounts of $Ba_2CuO_{2+\delta}$ ($<0.5\%$),[8] a clear indication that the solubility limit is close to 20%. The amount of oxygen of the original batches[8] was determined with an accuracy of $\Delta x=\pm 0.001$ using a volumetric technique[6] and found to oscillate between two oxygen content regions (phase *A*, samples $y=4$, 5, 7, 9, and 14 % corresponding to $x\cong 6.98$ and phase *B*, samples $y=2$, 10, 12, 15, and 17 % corresponding to $x\cong 6.96$), remaining always above the optimum doping ($6.960\leqslant x\leqslant 6.995$).[5,7] For $y=0.20$ there is no measurement of the oxygen content as there are indications for saturation of the Ca solubility.

The Raman spectra were recorded at room temperature and high hydrostatic pressures using a Jobin-Yvon T64000 triple spectrometer equipped with a liquid nitrogen cooled charge coupled device and a microscope lens of magnification $\times 100$ ($\times 40$ for the hydrostatic pressure measurements). High pressures were obtained by use of a Merrill-Bassett diamond anvil cell (DAC) for backscattering geometry manufactured by High Pressure Diamond Optics (HPDO). Although the samples were polycrystalline, individual microcrystallites were investigated. The 514.5 and 488.0 nm lines of an Ar^+ laser were used at a power less than 0.2 mW (or 0.4 mW for the high pressure measurements) on the sample. The local heating at the laser spot was estimated to be less than 10 K. The laser beam was focused on a single microcrystallite at a spot of diameter $1-2$ μm ($\times 100$ lens) or $3-5$ μm ($\times 40$ lens) and the scattering geometries were $y(zz)\bar{y}$ and $y(xx)\bar{y}$. In this notation, as usual, y and $\bar{y}$ define the direction of the incident and scattered light and the letters in parentheses the corresponding polarizations. Typical accumulation times were of the order of $1.5-3$ h (room temperature) or $3-6$ h (high pressures) and several microcrystallites were examined for the ambient measurements on each Ca concentration. Characteristic spectra for various Ca concentrations at ambient conditions are shown in Figs. 1 and 2 for the scattering geometries $y(zz)\bar{y}$ and $y(xx)\bar{y}$, respectively.

III. RESULTS

The Ca substitution for the smaller Y ion is expected to induce modifications in the Raman spectra related with the size of the ion at the rare earth (*R*) site.[13–15] Such changes include the shift of the B_{1g}-like and the apex modes and the appearance of new modes in the *xx*-polarization close in energy with the B_{1g}-like mode.[13,14] These modes have been attributed to a phase separation mechanism, which results in the formation of phases rich in the two rare earth ions and an intermediate mixed phase.[13] In the case of the Ca substitution additional effects arise from the charge difference between the trivalent Y and the divalent Ca ion. Such effects include the distribution of the additional carriers brought to the system and the modified local electric field in the CuO_2 planes from the Y/Ca and the Ba sites,[16] which can affect the possible phase separation of the compound.[13,14] In the following,

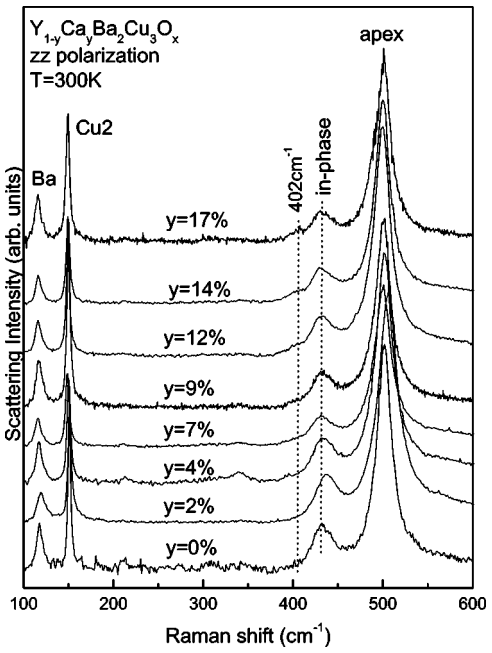

FIG. 1. Typical spectra from separate microcrystallites of $Y_{1-y}Ca_yBa_2Cu_3O_x$ compounds for selected Ca concentrations in the $y(zz)\bar{y}$ scattering geometry. A new mode appears at 402 cm^{-1}.

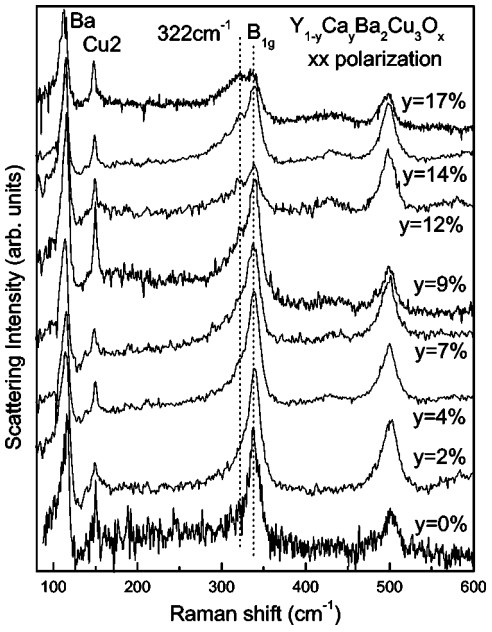

FIG. 2. The corresponding spectra of the same microcrystallite of each selected Ca concentration of Fig. 1 in the $y(xx)\bar{y}$ scattering geometry. A strong mode appears at 322 cm^{-1} with increasing intensity with Ca.

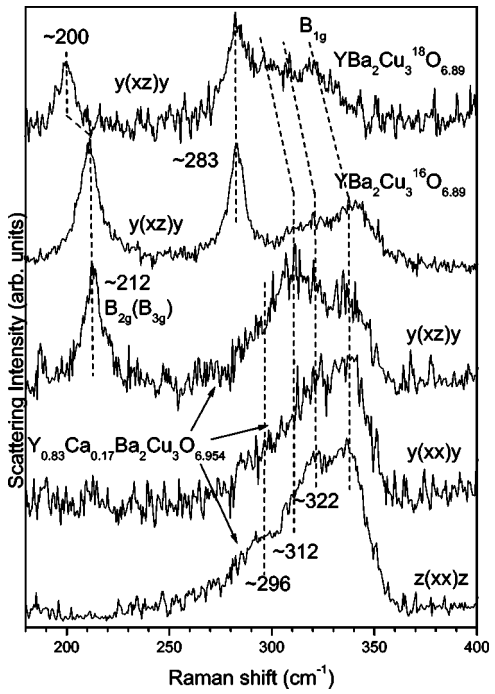

FIG. 3. Comparison of the spectra from YBa_2Cu_3 (Refs. 16 and 18) $O_{6.89}$ obtained in the $y(xz)\bar{y}$ scattering polarization with those of $Y_{0.83}Ca_{0.17}Ba_2Cu_3O_{6.954}$ in the $y(xz)\bar{y}$, $y(xx)\bar{y}$, and $z(xx)\bar{z}$ polarizations.

the Raman data from the Ca substituted compounds are compared with those of pure $YBa_2Cu_3O_x$ $(6.4<x<7)$ and rare earth substituted YBCO in order to extract information about those effects. To compare the pure YBCO with the Ca doped data, it is customary to use a common doping axis (doping induced either by oxygen or by Ca) where the scaling between the two doping routes is based on the experimental result that the same transition temperature is obtained either by overdoping by 20% Ca or by underdoping pure YBCO down to an oxygen concentration of 6.6.

In the *zz* scattering geometry (Fig. 1) the usual four A_g symmetry phonons appear, which are due to the vibrations of the Ba atoms, the Cu2 atoms, the in-phase vibrations of the plane oxygen atoms (O2,3), and those of the apical oxygen, all modes involving atomic motions along the *c* axis.[17] The spectra look very similar with the ones of pure YBCO, except for the gradual shift of the apex phonon and the appearance of a weak mode for high Ca concentrations at $\sim 402\ cm^{-1}$. In the *xx* geometry (Fig. 2) the previous phonons due to the Ba, Cu2, and the apical oxygen appear again, besides the out-of-phase vibrations of the O2,3 oxygen atoms with the characteristic B_{1g}-like symmetry.[17] The spectral region close to the B_{1g}-like phonon is considerably modified with the Ca substitution (Fig. 2) and two additional modes appear at ~ 298 and $\sim 322\ cm^{-1}$. In the cross polarization (*xz*) two more modes appear at ~ 312 and $\sim 212\ cm^{-1}$ (Fig. 3). The evolution of all these modes with the Ca doping is examined below.

A. B_{2g}, B_{3g} symmetry modes

The two modes at ~ 212 and $312\ cm^{-1}$ appear in the $y(xz)\bar{y}$ polarization with the B_{2g} or B_{3g} symmetry. In pure YBCO there is a phonon at $\sim 212\ cm^{-1}$, which has the same symmetry and shifts to lower energies upon isotopic substitution of ^{16}O by ^{18}O (Fig. 3).[18,19] In the Ca substituted samples it appears also in the crossed polarization at the same energy. It is therefore one of the modes that involve vibrations of the oxygen atoms, which are Raman active. Additional measurements we have carried out on site selective isotopic substitution for oxygen indicate that it involves the apex or the chain oxygen atoms.[20] Since in pure YBCO it is not modified by the loss of oxygen from the chains, it should involve the vibrations of the apex oxygen along the *ab* plane.[21] The $312\ cm^{-1}$ phonon, which is seen in the Ca compounds is covered by the surrounding modes and it is very difficult to be isolated and studied. A mode of similar symmetry, which does not shift with oxygen isotopic substitution and can thus not be an oxygen mode, appears at $\sim 283\ cm^{-1}$ in pure YBCO (Fig. 3), and must be some cation (Ba, Cu, or Y) mode. Ba can be excluded as its large mass is expected to shift related vibrational modes at lower energies. This mode of pure YBCO must then be related with vibrations of either of the Cu sites, or the Y atom [although the Cu(1) and Y modes are by symmetry only IR active]. If this is a Y mode, in the Y-Ca compounds the corresponding mode would be shifted to higher energies as a result of the different mass ratio of the two elements and in the case of the Ca 17% sample to $\sim 312\ cm^{-1}$. In any case, it does not substantially contribute to the spectra of the parallel polarizations (different scattering geometry) where a large part of our discussion is based.

B. Ba, Cu(2) phonons

The spectral characteristics (energy and width) of the Ba atom phonon do not show appreciable changes (Fig. 4), excluding any substantial amount of Ca substitution at the Ba site. The other mode of A_g symmetry, due to the vibrations of the Cu(2) atom of the CuO_2 planes, shows with Ca substitution a slight but clear softening by $\sim 2\ cm^{-1}$ while a hardening by $\sim 5\ cm^{-1}$ has been observed with the oxygen doping of pure YBCO (Fig. 4). The width of the Cu(2) phonon remains nearly constant within statistical error as in the pure YBCO (Fig. 4). The relative intensity of the two modes for both scattering geometries is presented in Fig. 5. In the *xx* polarization for the pure YBCO the relative intensity of the Cu(2) phonon gradually decreases with increasing oxygen concentration (Fig. 5) and the phonon is very weak in the overdoped compounds (Fig. 2 for $y=0$). This must be due to the increased screening as the carriers enter the CuO_2 planes. A linear fit of the data in Fig. 5 shows that the Ba mode disappears completely in pure YBCO for $x \cong 6.3$. This is roughly the oxygen concentration where the carrier injection to the CuO_2 planes is initiated.[22] In the Ca substituted samples with the high oxygen concentration ($y \geqslant 6.960$) the relative intensity remains constant or slightly increases (Fig. 5) and the Cu(2) phonon is more pronounced (Fig. 2) than in pure YBCO, despite the expected additional doping from Ca. This is an indication that the additional carriers do not behave in the same way as those from oxygen doping.

C. O2,3 in-phase phonon

In the *zz* polarization, the energy of the in-phase mode does not change with Ca while its bandwidth increases

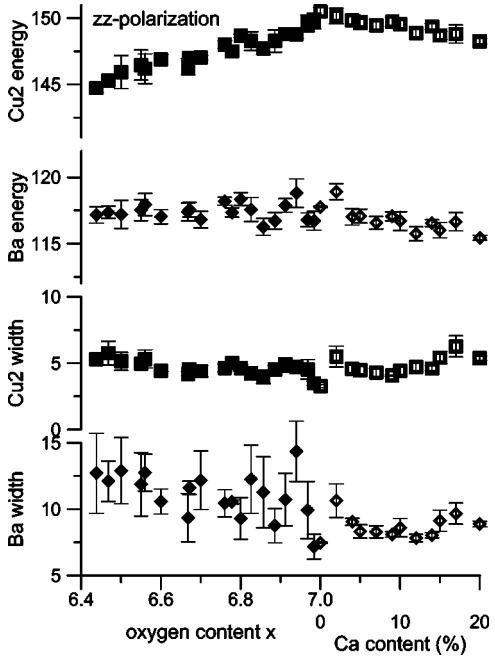

FIG. 4. The dependence of the energy and width (measured in cm^{-1}) of the Ba and the Cu(2) phonons on the oxygen concentration of $YBa_2Cu_3O_x$ (left side), and on the Ca content of $Y_{1-y}Ca_yBa_2Cu_3O_x$ (right side).

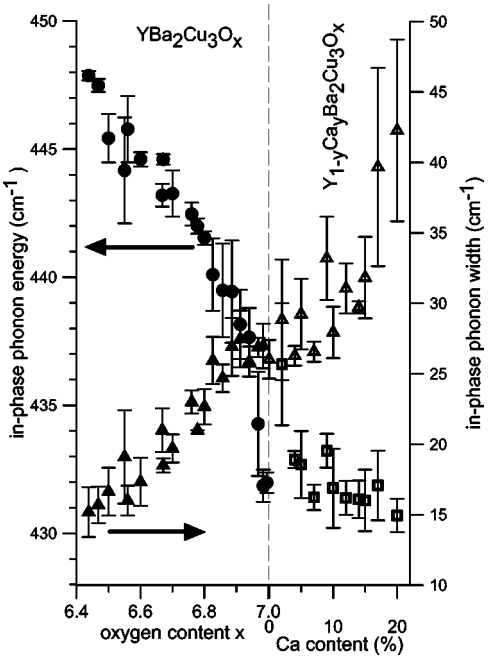

FIG. 6. The dependence of the in-phase phonon energy and width (measured in cm^{-1}) on the oxygen content of $YBa_2Cu_3O_x$ (left side) and the Ca doping of $Y_{1-y}Ca_yBa_2Cu_3O_x$ (right side).

gradually following the general trend of increase observed in pure YBCO with increasing amount of doping (Fig. 6). This increase of the total width of the in-phase band is partially due to the appearance of the weaker mode at lower energies ($\sim$402 cm^{-1}). In pure YBCO the in-phase phonon width increases almost linearly with doping in the orthorhombic phase (Fig. 6). The study of the spectral profile of this phonon for all Ca concentrations proves that three Lorentzians (at $\sim$402, $\sim$428, and $\sim$439 cm^{-1}) are necessary for the appropriate fit of all spectra. The two high energy modes are characteristic of the two phases from the change in the buckling in the overdoped pure YBCO compounds,[1] while the origin of the mode at 402 cm^{-1} is discussed below.

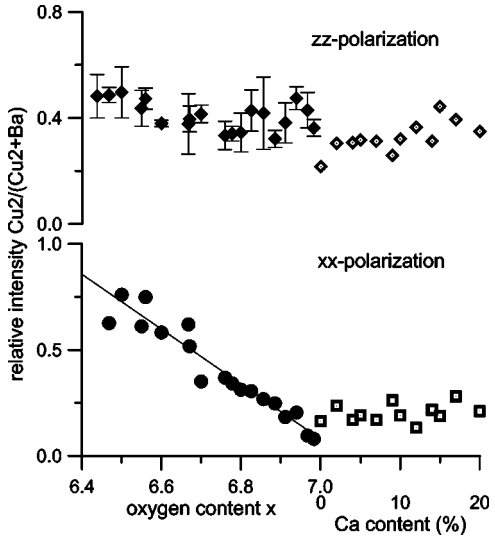

FIG. 5. The dependence of the relative intensity of the Cu(2) and Ba A_g-symmetry phonons on the oxygen concentration of $YBa_2Cu_3O_x$ (left side), and on the Ca content of $Y_{1-x}Ca_xBa_2Cu_3O_y$ (right side) for the two scattering polarizations. In the *xx* polarization the Ba line disappears completely for $x=6.3$, i.e., at the orthorhombic-to-tetragonal transition.

D. Apex phonon

The phonon energy of the apical oxygen decreases by $\sim$4 cm^{-1} with increasing amount of Ca while its width is not affected appreciably (Fig. 7). In some spectra with high amounts of Ca concentration the apex phonon seems to incorporate modes at $\sim$486 and $\sim$493 cm^{-1}. These correspond to the additional modes that appear in pure YBCO compounds with decreasing amount of oxygen.[18] If the apex phonon energy of the Ca substituted samples is compared with the results from underdoped $YBa_2Cu_3O_x$,[3] it is observed that the shift in energy follows quite symmetrically the doping concentration (Fig. 7). The decrease in its energy ($\sim$0.8%) is correlated with the increase of the interatomic distance Cu(2)-O_{apex} ($\sim$1.1%) presented in the inset of Fig. 7. This correlation should not be taken to imply that it is possible to deduce the degree of doping in the planes from the apex phonon energy. The behavior of the apex and the in-phase modes in Figs. 6 and 7 can be compared with the changes induced by other substitutions, when the distance of the apical oxygen atom to the CuO_2 planes is modified.[13–15] The substitution of 20% La or Pr (two ions of similar size to Ca) for Y induces an increase in energy of the apex phonon by $\sim$5 cm^{-1}.[13–15] At the same time the distance Cu(2)-O_{apex} decreases, which is opposite to the present situation. In those two rare earth or Ca substituted compounds with similar

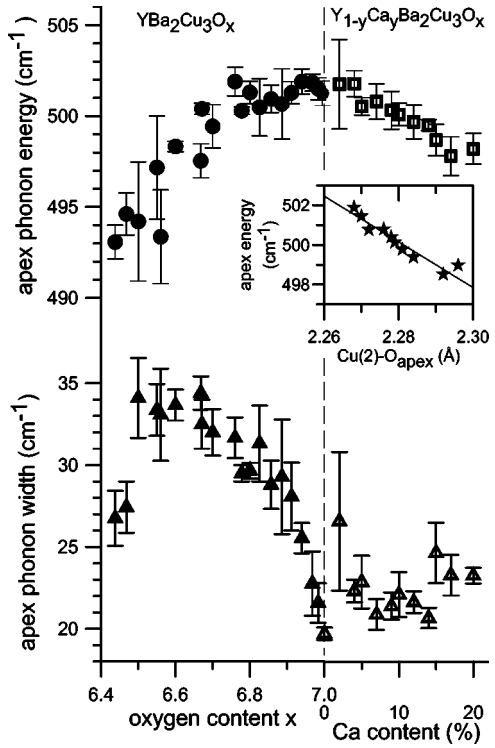

FIG. 7. The dependence of the apex phonon energy and width (measured in cm^{-1}) on the oxygen content of $YBa_2Cu_3O_x$ (left side), and the Ca doping of $Y_{1-x}Ca_xBa_2Cu_3O_y$ (right side). Inset: dependence of the apex phonon energy on the Cu(2)-O_{apex} interatomic distance.

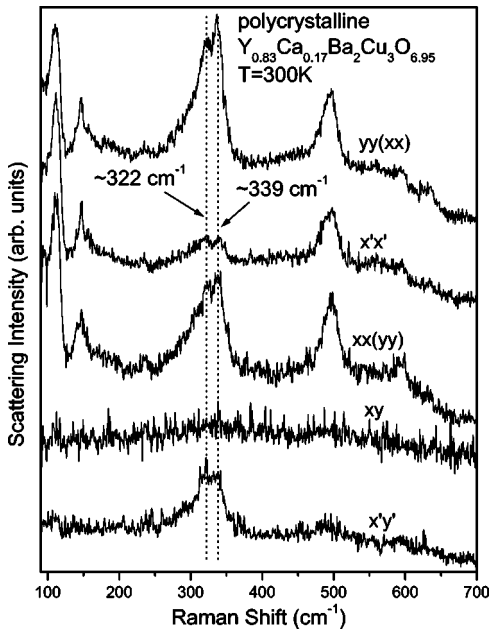

FIG. 8. Typical spectra of $Y_{0.83}Ca_{0.17}Ba_2Cu_3O_{7-\delta}$ at various scattering geometries to prove the B_{1g}-like symmetry character of the 322 cm^{-1} mode.

amount of oxygen, the decrease in T_c and doping is different, while the apex phonon energy either increases (La, Pr) or decreases (Ca). The observed decrease of the apex mode energy by Ca substitution indicates that the reduced charge of the Ca^{+2} ion as compared with the trivalent Y or the rare earths, counterbalances the effect of the increased ion size on the central cage, indirectly affecting the energy of the apex phonon.

E. B_{1g}-like phonon

The phonon of the out-of-phase vibrations of the O(2,3) plane oxygen atoms of approximate B_{1g} symmetry (in reality an A_g phonon in orthorhombic symmetry labeling), which appears in the $y(xx)y$ scattering geometry (Fig. 2), contains in addition to the well-known 340 cm^{-1} phonon, a mode at ~322 cm^{-1}. This mode becomes very strong in high Ca concentrations (Fig. 2), while a weak mode at ~296 cm^{-1} also appears (Figs. 2 and 3). Due to the presence of these additional modes, the spectral characteristics of the B_{1g}-like phonon cannot be determined accurately enough to draw conclusions. The total width of the phonon increases considerably, and the increased asymmetry reflects partially a Fano coupling with the excess carriers and partially originates from the appearance of the additional modes.

F. Mode at 296 cm^{-1}

The mode at ~296 cm^{-1} is very weak and appears in the parallel polarizations. One could assume that this mode corresponds to the B_{1g}-like phonon of a hypothetical phase $CaBa_2Cu_3O_x$. It is known that the energy of the B_{1g}-like mode is sensitive to the size of the rare earth, and mixed rare earth compounds can be composed of two or three phases.[13–15] The phonon energy of the corresponding peaks are associated with the pure compound of each rare earth and with a mixed system, which appears at an intermediate energy. A similar situation could exist in Fig. 2 and the mode at ~296 cm^{-1} might correspond to the pure Ca123 phase. This possibility is not supported by the rather large difference between its energy and the one anticipated for the Ca123 phase (~307 cm^{-1}) based on the rare earth data.[13–15] Since we cannot assign this mode to any other A_g symmetry phonon at the center of the Brillouin zone, it should be related with a phonon from the edges of the zone.

G. Mode at 322 cm^{-1}

The intensity of the mode at 322 cm^{-1} increases considerably with the Ca concentration while its energy remains independent of the amount of Ca (Fig. 2). In pure fully oxygenated YBCO compounds a very weak mode of similar energy has been observed under hydrostatic pressures and only in a mixed scattering geometry $zz+xx$.[23] This weak mode was soft, not shifting but gaining intensity with the application of hydrostatic pressure. As the chain oxygen atoms are removed the mode disappears and we have not observed it in single crystals under pressure of $YBa_2Cu_3O_{6.5}$. In order to investigate any connection of the strong mode at 322 cm^{-1} observed in the present Ca substituted samples with the soft one of pure YBCO, we have carried out complete scattering selection rules. It turns out that the mode has exactly the B_{1g}-like symmetry (Fig. 8) not agreeing with the symmetry of the soft phonon of pure YBCO. Furthermore,

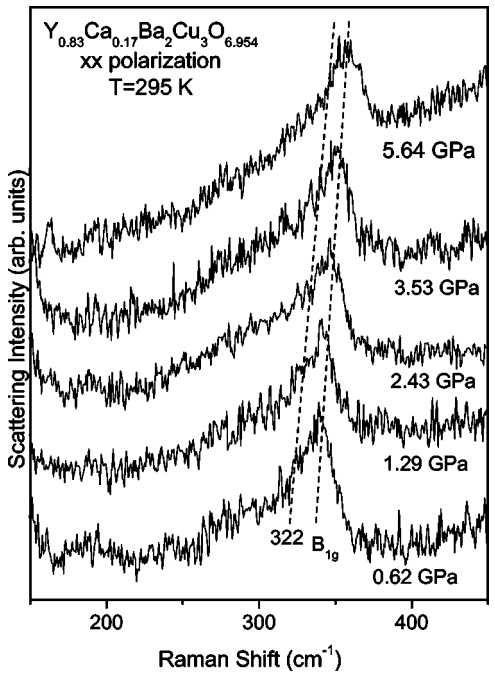

FIG. 9. Typical $y(xx)\bar{y}$ spectra at RT and high pressures for the $Y_{0.83}Ca_{0.17}Ba_2Cu_3O_{7-\delta}$ compound. It is clear that the 322 cm^{-1} mode tends to merge with the B_{1g}-like phonon at high pressures.

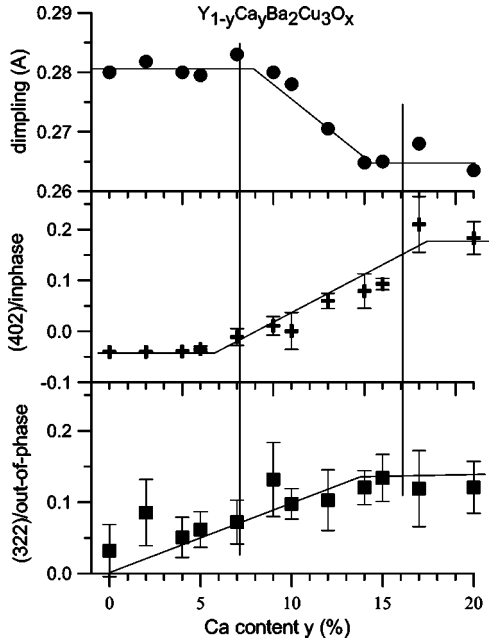

FIG. 10. Dependence of the relative intensity of the 322 cm^{-1} mode with respect to the B_{1g}-like band and the 402 cm^{-1} with respect the in-phase phonon on the Ca concentration. The CuO_2 plane dimpling (measured by EXAFS) is also shown for comparison.

we have studied under hydrostatic pressure the compound $Y_{0.83}Ca_{0.17}Ba_2Cu_3O_{7-\delta}$. The results shown in Fig. 9 prove that the mode at 322 cm^{-1} shifts with pressure contrary to the behavior of the soft mode of similar energy.[23] Another possibility is that the mode at 322 cm^{-1} be due to an IR active phonon that becomes Raman active by the Ca for Y substitution. If so, other rare earth substitutions for Y, which induce the same disorder at the Y site should activate this mode. But no indications for such mode at a fixed energy have been observed up to now.[13–15]

In rare earth substitutions for Y an intermediate phase appears ($Y_{1-y}R_yBa_2Cu_3O_{7-\delta}$) with increasing intensity and modified energy that depends on the amount of rare earth.[13–15] This phase is created mainly by the difference in the ion size and not by the mass difference between Y and *R*.[13–15] In a mixed compound with homogeneous distribution of the substituting ions, it is possible to observe either of the so-called one- or two-mode behavior. In the former case, the phonon related with the substituted ion shifts continuously with the amount of substitution. Such behavior has not been observed with the present mode. In the case of a two-mode behavior, independent modes appear characteristic of the two end compositions, which for Ca substitution could be the CaBCO and YBCO phases. But the energy of the 322 cm^{-1} mode does not agree with the general trend of the B_{1g}-like phonon dependence on the ion size for the rare earths.[13] Nevertheless, some effect from the charge difference between Y and Ca cannot be excluded.

Finally, one could have a separation into phases like YBCO, CaBCO, and a mixed one (Y-Ca)BCO, as observed in the rare earth substitutions for Y.[13–15] For low amounts of *R* substitutions for Y (below ~20%), it is common not to observe the pure phase of *R*BCO.[15] The constant value of the mode energy would then imply a constant ratio Y, Ca in this mixed intermediate phase. Based on the ion size dependence of the B_{1g}-like phonon energy[13–15] we calculate that the energy of the ~322 cm^{-1} mode corresponds to the mixed $Y_{0.5}Ca_{0.5}Ba_2Cu_3O_{7-\delta}$ phase with approximately equal amounts of Ca and Y atoms similar to the one suggested by EXAFS measurements.[10] No matter what is the exact relative amount of Ca to Y in this mixed phase, the important result is the independence of this mode energy from the Ca concentration. This implies that only the volume fraction of this mixed phase is modified with the addition of Ca.

H. 402 cm^{-1} mode

Close to the in-phase vibrations of the O(2,3) oxygen atoms, an additional weak A_g symmetry mode appears at an energy of ~402 cm^{-1} (Figs. 1 and 11). As in the case of the 322 cm^{-1} mode, the intensity of this weak mode also increases with the amount of Ca (Fig. 10) and could correspond to another phonon activated by the Ca substitution for Y. It does not seem to correspond to any of the IR-active phonons that have been observed or predicted by lattice dynamic calculations.[21] The ~402 cm^{-1} mode has been observed also in very low oxygen concentration $YBa_2Cu_3O_x$ ($x<6.4$) samples where other phases related to the formation of superstructures are created (Fig. 11). We therefore attribute this mode to a phonon from the edge of the Brillouin zone activated by the formation of a superstructure and gaining intensity with the Ca substitution.

IV. DISCUSSION

One question to be addressed is the possible substitution of Ca for Ba. As explained above, this substitution would be

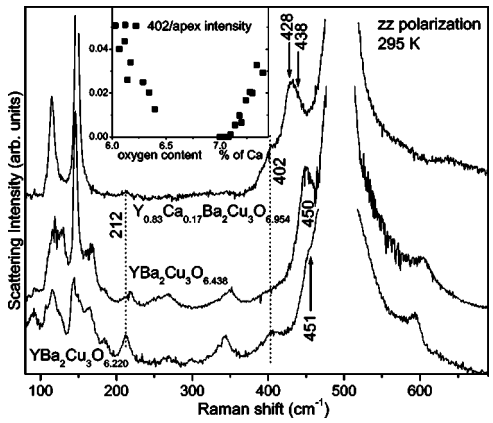

FIG. 11. Comparison of the spectra from $YBa_2Cu_3O_{6.220}$, $YBa_2Cu_3O_{6.438}$, and $Y_{0.83}Ca_{0.17}Ba_2Cu_3O_{6.954}$ obtained in the $y(zz)\bar{y}$ polarization. Inset: the relative intensity of the 402 cm^{-1} mode to the apex phonon for $YBa_2Cu_3O_x$ and $Y_{1-y}Ca_yBa_2Cu_3O_x$.

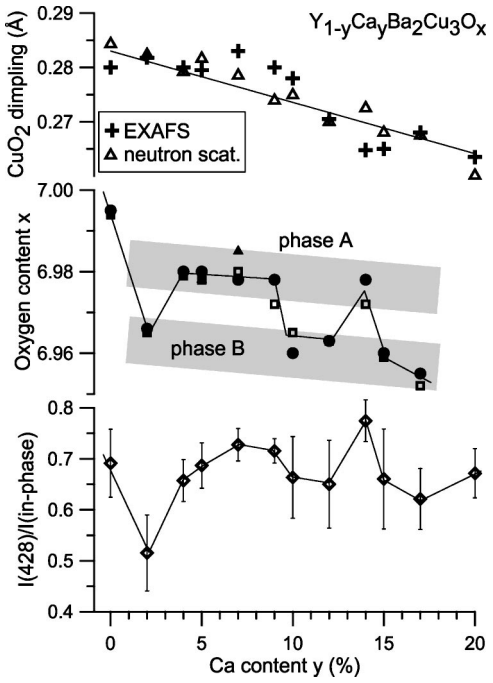

FIG. 12. Quantities versus Ca content. Top panel: CuO_2 plane dimpling as measured by neutron scattering (Ref. 8) and EXAFS (Ref. 10). The straight line is the expected reduction of the dimpling due to the reduced charge of Ca^{+2} substituting for Y^{+3} (see text). Middle panel: Oxygen content—different symbols correspond to different sets of measurements. Bottom panel: relative intensity of the Raman 428 cm^{-1} line with respect to the total in-phase band. Note the scaling with the oxygen content and not with Ca or the amount of dimpling.

expected to reveal itself in the Raman spectra in either one of the two following ways. In the one-mode behavior, the phonon corresponding to Ba should shift continuously with increasing amount of Ca up to an energy of 123 cm^{-1} (for $y=0.20$ and assuming the total amount of available Ca enters the Ba site), in a manner analogous to the case of $SmBa_{2-y}Sr_yCu_3O_{7-\delta}$.[24] A smaller amount of substitution would induce of course a smaller shift. In the two-mode behavior a new mode at $\sim$220 cm^{-1} would appear with intensity increasing along with x. The fact is (Fig. 4) that neither the energy nor the width of the Ba phonon increases continuously with increasing Ca content (one-mode scenario). Furthermore, the intensity of the $\sim$212 cm^{-1} line does not increase systematically with Ca concentration, its symmetry is different from that of the Ba atom and therefore this mode cannot be attributed to Ca (two-mode scenario). Therefore, the Raman results suggest that if it is assumed that some Ca substitutes for Ba,[25] the amount would be small. This is in very good agreement with the neutron diffraction[8] and EXAFS (Refs. 10 and 11) work, carried out in samples from the same batches, which excludes substitution more than 3%.

In pure YBCO the increase of doping with the oxygen concentration induces a rapid increase in the intensity of the Ba phonon (in the *xx* scattering polarization). At the same time the intensity of the Cu(2) atom phonon decreases considerably, so that the phonon can hardly be seen (Fig. 2, $y=0$) in the overdoped region.[18] This behavior has been attributed to the redistribution of the carriers, which are introduced by the chain oxygen doping to the CuO_2 planes according to the scheme of Ref. 22. With the additional doping by Ca the Cu(2) phonon intensity increases instead of further decreasing, while the Ba phonon intensity remains unaffected (Fig. 2). This is an indication that the carriers introduced by Ca reside *neither at the CuO_2 nor at the BaO planes*. This can happen if *the Ca atoms remain isolated acting as pinning centers for the excess carriers*.[10]

Turning now to the spectral modifications, differences are observed between the effect of doping with oxygen and Ca. In the case of the in-phase mode, its energy is rather insensitive to the amount of Ca although in pure $YBa_2Cu_3O_x$ the energy decreases almost linearly until $x\cong 6.92$, where the softening of the mode occurs (Fig. 6).[1] The width of this mode, which in the orthorhombic phase increases with oxygen doping, shows a similar increase with Ca doping. Since the mode at $\sim$402 cm^{-1} appears with increasing amount of Ca (Fig. 10), we believe that the increase of the in-phase phonon width is mostly due to the development of this mode.

In the overdoped oxygen concentration region of $YBa_2Cu_3O_x$ it was found that the in-phase mode consists of two peaks (428 and 438 cm^{-1}), which originate from the coexistence of two phases that differ in the amount of the CuO_2 dimpling.[1] A similar structure of the in-phase mode can be observed in the Ca compounds, which are fully oxidized. The deconvolution of the in-phase phonon into two bands with peak positions at 428 and 438 cm^{-1} (Fig. 11) proves that the relative intensity of the two phases is not correlated with the Ca content but with the small changes in the amount of oxygen (Fig. 12). As seen in Fig. 6, for the whole range of Ca doping the in-phase phonon remains practically constant in energy implying that the softening of the in-phase phonon in the oxygen overdoped region cannot be related with the total amount of the carriers in the compound. Neither can it be related with the dimpling of the CuO_2 planes, since the dimpling decreases with Ca (Refs. 8 and 10) (Fig. 12) while the in-phase mode energy remains constant (Fig. 6). It is clear from Fig. 12 that there is a decrease

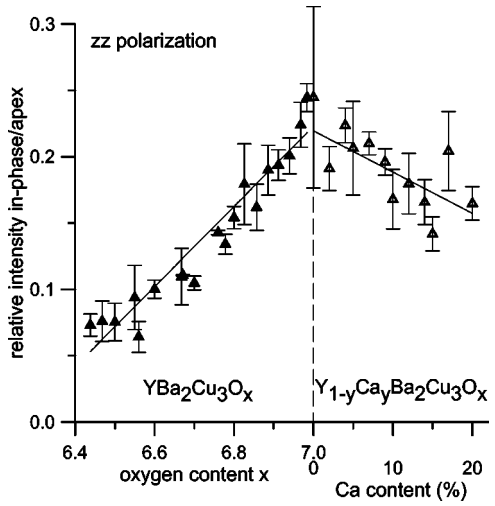

FIG. 13. The dependence of the relative intensity of the in-phase to the apex phonons on the oxygen concentration of $YBa_2Cu_3O_x$ (left side), and on the Ca content of $Y_{1-y}Ca_yBa_2Cu_3O_x$ (right side). Straight lines are best linear fits.

of the dimpling with the Ca substitution, although the relative intensity of the two components of the in-phase mode oscillates between two values that map closely the modifications in the oxygen content.

The dimpling measured by EXAFS shows an abnormal dependence on Ca (Fig. 10). This behavior is not clearly seen in the neutron scattering, though on the average the two sets of measurements agree very well (Fig. 12). A reduction in the dimpling is expected from the modification of the charge at the Y/Ca site.[16] Assuming a linear dependence the dimpling d will follow the equation $d(y)=d_o[3(1-y)+2y]/3=d_o[1-y/3]$ (straight line in Fig. 12). No additional carriers are supposed to reside in the CuO_2 planes in this simple approximation. Although this elementary model cannot predict the unexpected behavior of the dimpling measured by EXAFS, the agreement between the average dimpling and the charge reduction is quite good. This would imply that the reduction of the dimpling can be attributed solely to the decrease of the local electric field from the substitution of Ca^{+2} for Y^{+3}.[26] At the same time, it would suggest that the Ca substitution does not increase the amount of carriers in the CuO_2 planes and would explain the insensitivity of the in-phase phonon energy on the amount of Ca doping (Fig. 6), as the excessive carriers would not be introduced in the CuO_2 planes of the YBCO phase. Based on the behavior of this mode on (oxygen or Ca) doping, one can assume that the in-phase energy is related with the amount of carriers in the planes which, in connection with the strength of the local electric field, induces the CuO_2 dimpling.[26] This assumption agrees with the modifications of the spectral characteristics of the in-phase mode observed in pure YBCO.[27]

Figure 13 shows the dependence of the relative intensity of the in-phase to the apex mode for the pure YBCO and the Ca doped samples. For the pure YBCO the relative intensity increases with oxygen doping and then decreases with Ca. Besides it shows deviations from linearity for at least two characteristic oxygen concentrations, i.e., for $x\cong 6.4$ and 6.95. Above the first concentration the system becomes orthorhombic[7] and the carriers start populating the CuO_2 planes.[22] The $x\cong 6.95$ is the boundary to the overdoping where a sudden increase of the dimpling has been measured by EXAFS (Ref. 1) and the relative intensity increases also suddenly. For the Ca doping, the dimpling measured by neutron[8] or EXAFS (Ref. 10) decreases again as depicted in Fig. 12. As discussed, the dimpling of the CuO_2 planes can be related to the local electric field produced by the different valence of the Y/Ca and the Ba ions and the amount of carriers in the CuO_2 planes.[26] It is expected to decrease as a result of either the decreasing charge difference between the sites of Y and Ba, as the substitution of Ca^{+2} for Y^{+3} proceeds, or the reduction of the carriers in the planes. In pure YBCO the sudden increase of the dimpling at the optimal to overdoped region should therefore indicate a sudden increase of the carriers in the planes. The relative intensity of the in-phase mode seems to follow closely the changes of the dimpling in both the pure YBCO and in the Ca substituted compounds, actually probing the combined effect of the local electric field and the amount of carriers in the CuO_2 planes.

Focusing to the fine details uncovered by EXAFS one can observe stepwise changes in the dimpling at $\sim$7% and $\sim$14% (Fig. 10). Similar stepwise changes at approximately the same Ca concentrations are observed in the relative intensity of the mode at $\sim$402 cm^{-1} with respect to the in-phase phonon (Fig. 10). The phonon at $\sim$402 cm^{-1} appears only at Ca concentrations $\geqslant$6% and its relative intensity reaches a saturation level at $\sim$17%. The same mode has been detected also in the tetragonal phase of pure $YBa_2Cu_3O_x$ (Fig. 11), where the relative intensity decreases with doping in a symmetrical way as it increases with the Ca concentration (inset of Fig. 11). We could not assign this mode to a specific phonon at the center of the Brillouin zone of the pure compound. Since this mode appears also in the tetragonal phase of pure YBCO (Fig. 11), an explanation could be the association of the $\sim$402 cm^{-1} band with a phonon from an edge of the Brillouin zone, which becomes Raman active as a result of the formation of a superstructure. The presence of weak bands at $\sim$493 and $\sim$486 cm^{-1} in the apex phonon of the Ca compounds can be attributed also to the formation of superstructure phases similar to the ones that appear in pure YBCO.[28] In $YBa_2Cu_3O_x$ the band at $\sim$486 cm^{-1} dominates the apex phonon spectrum for $x\sim 6.15$,[27] and its association with the S point of the Brillouin zone[28] would agree also with the appearance of the $\sim$402 cm^{-1} mode in pure YBCO for $x\sim 6.22$ but not for $x\sim 6.438$ (Fig. 11). It is thus conceivable that the $\sim$402 cm^{-1} line is related to the development of a tetragonal phase different from the O-II phase in both materials. Furthermore, this assignment can explain the correlation of the relative intensity of the $\sim$402 cm^{-1} mode (Fig. 10) with the EXAFS measurements and the changes of the dimpling, since these changes have been associated with the formation of crosslike clusters.[10] Besides, it supports the assignment of the weak mode at $\sim$296 cm^{-1} to a phonon from the edge of the Brillouin zone.

The origin of the mode at $\sim$322 cm^{-1} has been discussed above and the phonon can be attributed either to a two-mode behavior of the mixed $Y_{1-y}Ca_yBa_2Cu_3O_x$ compound or to a separation into the phase of pure YBCO and another mixed

of $Y_{0.5}Ca_{0.5}Ba_2Cu_3O_{7-\delta}$ with roughly equal amounts of Ca and Y. The former case appears in mixed compounds $A_{1-x}B_xC$ when there is a large difference between the masses of the *A*, *B* ions and the two modes correspond to the *AB* and *BC* end compounds. In rare earth substitutions for Y, no sign of a two-mode behavior has been detected when the mass difference between Y and the rare earth is the largest ($Y_{1-y}Lu_yBa_2Cu_3O_x$), but the intermediate mode appears only when the difference between the size of the two ions reach a critical value.[13] Besides, the energy of the mode at $\sim 322\ cm^{-1}$ does not fit with the ion size of Ca and the general trend of the B_{1g}-like phonon dependence on the rare earth.[13]

The case of phase separation is typical for rare earth substitutions for Y and is driven mainly by the different ion size of the rare earth and the Y atoms.[13–15] It is likely that the same happens by the larger Ca ion substituting for Y, which can induce a separation into phases. Both the intermediate phase marked by the peak at $322\ cm^{-1}$ and the peak at $\sim 340\ cm^{-1}$ correspond to the approximate B_{1g}-symmetry phonon and remain fixed in energy, independently of the amount of Ca (Fig. 2). The fit of the $250-400\ cm^{-1}$ spectral region by Fano shaped bands shows the dependence of the relative intensity of the $\sim 322\ cm^{-1}$ mode to the B_{1g}-like phonon of pure YBCO (Fig. 10). Although the fit introduces an uncertainty in the determination of the relative intensity of the mode, it is clear that the phase responsible for this mode at $\sim 322\ cm^{-1}$ increases up to $\sim 14-15\,\%$ Ca and then remains constant. This is roughly the concentration where there is a marked change in the dimpling measured by EXAFS (Fig. 10) and a sudden decrease of the T_{c1} (see Ref. 7). The saturation of the mode intensity and the corresponding intermediate phase may originate from the Ca solubility limit in the compound ($\sim 20\%$).

Taking into consideration the results from EXAFS,[10] which "see" no Ca ion as a first neighbor to another Ca, and the Raman data supporting a mixed phase with equal amounts of Y and Ca, one concludes that this intermediate phase must be related with a checkerboard distribution of the Ca and Y atoms. The fact that the mixed phase can be detected by Raman spectroscopy indicates a size of at least several unit cells, while the absence of any sign for such a phase from neutron scattering measurements[8] sets an upper limit of an order of magnitude higher from that of Raman. In such a scheme of phase separation, the spectroscopic modifications discussed above show that the additional charges brought on by Ca are not homogeneously distributed as the corresponding carriers of a pure homogeneous, optimally doped YBCO system.[29] The formation of an intermediate phase with the Ca ions staying apart fully agrees with the results of EXAFS and the corresponding model, where the additional charges introduced by Ca are somehow trapped into the intermediate phase.[10] This phase may have a different T_c supporting the existence of two transition temperatures of the compounds.[7]

La^{+3} and Ca^{+2} are two ions with almost the same size. In both cases of ion substitution for Y, the Raman spectra show a peak at a lower energy to that of the B_{1g}-like phonon of pure YBCO. In $Y_{1-y}La_yBa_2Cu_3O_{7-\delta}$ the peak position of this mode corresponds to a hypothetical mixed Y-La123 phase,

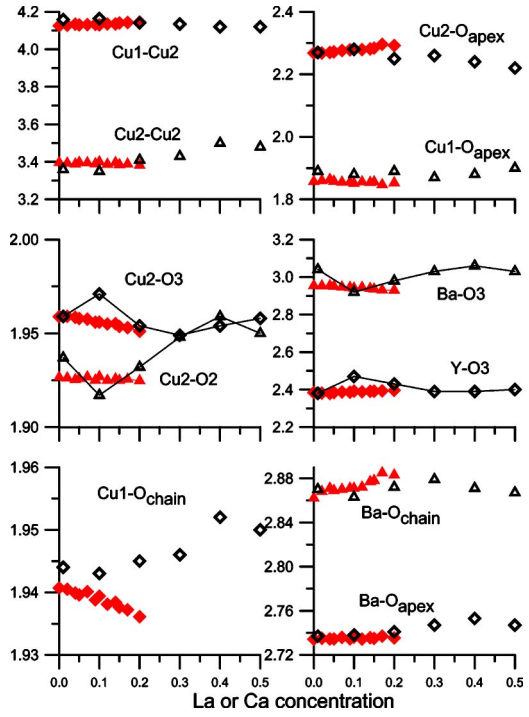

FIG. 14. Comparison of the dependence of several interatomic distances on the amount of Ca (Ref. 8) or La (Ref. 15) substitution for Y. It is seen that in the case of Ca substitution, only the distance between the Cu to the oxygen of the chains is modified, affecting also the *b* axis (not presented).

which differs only little from the nominal amount of substitution.[15] For $Y_{1-y}Ca_yBa_2Cu_3O_{7-\delta}$ this peak has an energy, which corresponds to constant, roughly equal, amounts of Y and Ca. If this mode derives from an intermediate phase, it is clear that there is an additional factor that affects the formation of this intermediate phase besides the ion size (volume) effect. Figure 14 shows the dependence of the interatomic distances on the amount of La (Ref. 15) or Ca (Ref. 8) substitution. It is seen that all structural parameters behave in a similar way except the Cu(1)-O_{chain} distance along the chains, where instead of an increase with La we observe a decrease in the case of Ca. This decrease affects also the *b* axis, which also decreases with Ca substitution.[8] This might be related with a new ordering of the chains, which affects the average Cu(1)-O_{chain} distances (or the *b* axis). A random breaking of the chains is not supported by our Raman measurements, since it would alter the inversion symmetry around the O_{chain} atoms. The related phonon from these atoms would become Raman active and it should have been observed in the *zz*-symmetry spectra with energy $\sim 600\ cm^{-1}$ [Fig. 1(a)]. If the reduction of the Cu(1)-O_{chain} distance with the addition of Ca could be related with a breaking of the chains, a regular orientation should have been created like a zigzag form around the Ca sites in the intermediate phase only.

Recently it was found that in $Gd:Y_{1-y}Ca_yBa_2Cu_3O_6$ with very small amounts of Gd and Ca substitution for Y ($y=0.008$), the carriers are not localized at the Ca sites[30] as first neighbors to the Gd. In this lightly doped antiferromagnetic environment, at low temperatures, the easy magnetic

axis is along the [110] direction changing gradually to the usual [100] between 10 and 100 K and this has been interpreted as hole ordering.[30] In our optimally doped compounds, there is no magnetic ordering, but still there might be a different ordering of the chains, at least around the Ca sites. This could result from the internal strain and the changes in the dimpling, in connection with the carrier distribution. It should be remarked that Gd atom is a medium size ion between Y^{+3} and Ca^{+2}. Therefore, a smaller (volume) strain is expected around Gd than around the Ca ion. It is unclear how this could affect the localization of the carriers around the Ca sites. In any case, the two sets of data do not seem to be in conflict, but they show a tendency of the compound for phase separation, which is related with charge ordering.

V. CONCLUSIONS

The slight modifications in the Raman spectra and the appearance of additional modes induced by the Ca substitution are correlated with characteristic changes in the local structure, the distribution of the excess carriers introduced by the Ca doping, and the formation of phases. The variation of the spectral profile of the in-phase vibrations of the O(2,3) oxygen atoms supports the coexistence of two phases in the underdoped-overdoped region of pure YBCO. The one-to-one correlation of the relative intensity of each phase with the amount of oxygen indicates that the formation of these two phases depends only on the amount of oxygen and not on the total carriers and the Ca concentration. The amount of dimpling seems to follow the reduction of the magnitude of the electric field produced by the unequal charges at the Ba^{+2} and the Y^{+3}/Ca^{+2} sites but must also be related with the amount of carriers in the superconducting planes. Additional modes, which appear at some critical Ca concentration, are correlated with the modifications of the dimpling of the CuO_2 planes and the formation of superstructures, attributed to the special way Ca is dissolved in the compound. It seems that the influence on the physical properties induced by the Ca-introduced excess doping is related with a phase separation and an inhomogeneous carrier distribution in the system, which is also related with the dimpling of the CuO_2 planes.

ACKNOWLEDGMENT

The authors thank Professor J. Röhler for fruitful discussions.

[1] E. Kaldis, J. Röhler, E. Liarokapis, N. Poulakis, K. Conder, and P. W. Loeffen, Phys. Rev. Lett. **79**, 4894 (1997).
[2] N. Poulakis, D. Palles, E. Liarokapis, K. Conder, E. Kaldis, and K. A. Müller, Phys. Rev. B **53**, R534 (1996).
[3] D. Palles, D. Lampakis, N. Poulakis, K. Conder, E. Kaldis, and E. Liarokapis, Physica C **282–287**, 1051 (1997).
[4] J. B. Torrance, Y. Tokura, A. I. Nazzal, A. Bezinge, T. C. Huang, and S. S. P. Parkin, Phys. Rev. Lett. **61**, 1127 (1988).
[5] E. Kaldis, in *Workshop on High-Tc Superconductivity 1996: Ten Years after the Discovery*, edited by E. Kaldis, E. Liarokapis, and K. A. Müller, NATO Advanced Studies Institute, Series E: Applied Sciences Vol. 343 (Kluwer Academic, Dordrecht, The Netherlands, 1997), pp. 411–446.
[6] K. Conder, S. Rusiecki, and E. Kaldis, Mater. Res. Bull. **24**, 581 (1989).
[7] E. Kaldis, in *Handbook of Physics and Chemistry of the Rare Earths*, edited by K. Gschneider, L. Eyring, and B. Mapple (Elsevier, New York, 2001), Vol. 31, pp. 1–186.
[8] G. Böttger, I. Mangelschots, E. Kaldis, P. Fischer, Ch. Kruger, and F. Fauth, J. Phys.: Condens. Matter **8**, 8889 (1996).
[9] J. Röhler, P. W. Loeffen, S. Mullender, K. Conder, and E. Kaldis, in *Workshop on High-Tc Superconductivity 1996: Ten Years after the Discovery*, edited by E. Kaldis, E. Liarokapis, and K. A. Müller, NATO Advanced Studies Institute, Series E: Applied Sciences Vol. 343 (Kluwer Academic, Dordrecht, The Netherlands, 1997), pp. 469–502.
[10] J. Röhler, C. Friedrich, T. Granzow, E. Kaldis, and G. Böttger, in *High Temperature Superconductivity*, edited by S. E. Barnes, AIP Conf. Proc. No. 483 (AIP, New York, 1999), pp. 320–323.
[11] J. Röhler, E. Rose, J. B. Philip, T. Lipinski, G. Böttger, and E. Kaldis, Annual Report HASYLAB, 1999 (unpublished).
[12] D. Palles, D. Lampakis, G. Böttger, E. Liarokapis, and E. Kaldis, Physica C **341–348**, 2149 (2000).
[13] G. Bogachev, M. Abrashev, M. Iliev, N. Poulakis, E. Liarokapis, C. Mitros, A. Koufoudakis, and V. Psycharis, Phys. Rev. B **49**, 12 151 (1994).
[14] M. Calamiotou, A. Gantis, D. Palles, D. Lampakis, E. Liarokapis, and A. Koufoudakis, Phys. Rev. B **58**, 15 238 (1998).
[15] A. Gantis, M. Calamiotou, D. Palles, D. Lampakis, and E. Liarokapis, Phys. Rev. B **68**, 064502 (2003).
[16] S.-G. Eriksson, C. Ström, P. Berastegui, M. Osada, M. Kakihana, M. Käll, and L. Börjesson, Physica C **235–240**, 389 (1994).
[17] C. Thomsen and M. Cardona, in *Physical Properties of High Temperature Superconductors*, edited by D. M. Ginsberg (World Scientific, Singapore, 1989), p. 409.
[18] D. Palles, Ph.D. thesis, National Technical University of Athens, 2000.
[19] D. Palles, N. Poulakis, E. Liarokapis, K. Conder, E. Kaldis, and K. A. Müller, Phys. Rev. B **54**, 6721 (1996).
[20] D. Zech, H. Keller, K. Conder, E. Kaldis, E. Liarokapis, N. Poulakis, and K. A. Müller, Nature (London) **371**, 681 (1994).
[21] A. P. Litvinchuk, C. Thomsen, and M. Cardona, in *High Temperature Superconductors*, edited by D. M. Ginsberg (World Scientific, Singapore, 1994), Vol. IV, p. 375.
[22] R. J. Cava, A. W. Hewat, E. A. Batlogg, M. Marezio, K. M. Rabe, J. J. Krajewski, W. F. Peck, Jr., and L. W. Lupp, Jr., Physica C **165**, 419 (1990).
[23] K. Syassen, M. Hanfland, K. Strossner, M. Holtz, W. Kress, M. Cardona, U. Schroder, J. Prade, A. D. Kulkarni, and F. W. de Wette, Physica C **153–155**, 264 (1988).
[24] V. Psycharis, C. Mitros, A. Koufoudakis, H. Gamari-Seale, D.

Niarchos, N. Kalitsounakis, N. Poulakis, D. Palles, and E. Liarokapis, Physica C **267**, 211 (1996).
[25] J. L. Tallon, C. Bernhard, H. Shaked, R. L. Hitterman, and J. D. Jorgensen, Phys. Rev. B **51**, R12 911 (1995).
[26] T. P. Devereaux, A. Virosztek, and A. Zawadowski, Phys. Rev. B **51**, 505 (1995).
[27] E. Liarokapis, D. Palles, K. Conder, and E. Kaldis, J. Raman Spectrosc. **32**, 821 (2001).
[28] L. Pintsovius and W. Reichardt, *Properties of High Temperature Superconductors* (World Scientific, Singapore, 1994), Vol. IV, p. 295.
[29] M. Merz, N. Nücker, P. Schweiss, S. Schuppler, C. T. Chen, V. Chakarian, J. Freeland, Y. U. Idzerda, M. Kläser, G. Müller-Vogt, and Th. Wolf, Phys. Rev. Lett. **80**, 5192 (1998).
[30] A. Janossy, T. Feher, and A. Erb, Phys. Rev. Lett. **91**, 177001 (2003).